Modified Carrier-Based Over-Modulation Technique for Improved Switching Performance of Multilevel Converters

Md. Ashib Rahman*, *Member, IEEE*, Md. Rabiul Islam*, *Senior Member, IEEE*, Youguang Guo[†], *Senior Member, IEEE*, Jianguo Zhu[†], *Senior Member, IEEE* and Gang Lei[†], *Member, IEEE*
*Rajshahi University of Engineering & Technology (RUET), Rajshahi–6204, Bangladesh
[†]University of Technology Sydney, New South Wales 2007, Australia
Email: m.rahman.bd@ieee.org, rabiulbd@hotmail.com, youguang.guo-1@uts.edu.au, jianguo.zhu@uts.edu.au and
gang.lei@uts.edu.au

Abstract—A modified over-modulation (OVM) scheme with phase disposed carriers to improve switching performance of cascaded H-bridge multilevel converter is depicted in this article. With the regular OVM techniques, pulse dropping region has higher conduction loss, greater signal distortion and voltage gain. In the proposed OVM method, the switching and conduction loss scenario is improved with lower harmonic distortion. Also, the voltage gain can be increased up to limited range. Four types of reference signals, such as pure sinusoidal signal, sinusoidal 60° bus clamped signal, third harmonic injected signal and third harmonic injected 60° bus clamped signal are used to investigate the overall performance with the proposed OVM method. The OVM technique is applied to a 3.0 kV, 120 kW, 5-level cascaded H-bridge converter and simulated in MATLAB/Simulink environment. The results demonstrate reduced output harmonic distortion, increased voltage gain, lower switching and conduction loss as well as improved efficiency on the whole.

Keywords—Cascaded H-bridge, multilevel converter, over-modulation, switching and conduction loss.

I. INTRODUCTION

Since the first introduction of multilevel converters (MLCs) in 1975 [1], they (2.3–30 kV, 0.3–32 MVA) are replacing the conventional 2 or 3-level converters (3-LCs) and becoming industry standard for the implementation of most modernized, medium (0.1–5.0 MW) to large scale (6.0–50 MW) micro-grid system. The MLC can be designed to operate in particular higher voltage levels which completely eliminates the use of any low frequency, heavy step-up transformers (50–70% of converter weight and 30–50% of drive size are characterized by transformer [2]) and removes bulky filtering circuitry (43-L MLC) [3]. In this work, the cascaded H-bridge (CHB) MLC is selected for its superior qualities. Since the first appearance of CHB in 1988 [4], this technology is standardized with a power range of 0.15–120 MW and frequencies up to 330 Hz [5]. Currently the CHB is applied in MV, high power drive markets with maximum rating of 13.8 kV, 1400 A and 31.0 MVA [6].

A modified over-modulation (OVM) technique for the MLC is investigated in this article. OVM method is a special type of pulse width modulation (PWM) where the target reference signal is raised higher than the carrier signals. Usually in low modulation region, the fundamental voltage of the modulator increases linearly with the modulation index (MI), but in OVM region this linearity breaks down and the pulse dropping region starts to occur. Mainly two types of implementation processes are given priority; direct digital PWM, also known as space-vector PWM (SVPWM) and carrier interaction PWM [7]. Regular OVM technique possesses some adverse effects on converters [8], such as:

- Low order harmonics or sub-carrier harmonic generation in the modulator output voltage and current (low level base-band distortion);
- Significant reduction of the gain of fundamental voltage component;
- Loss of linearity of fundamental voltage with modulation index; and
- Abrupt dropping of switch pulses.

Those so-called negative features make the OVM technique avoidable in regular realm of modulation. However, in OVM, the fundamental voltage component can be increased within a reasonable limit, keeping an eye to restrict harmonic contents in controllable range. This property helps converters and variable speed drives to exhibit reliable performance in the occurrence of dc bus voltage deviation and abrupt fault conditions [8], to utilize rated power [9] and to reduce overall converter cost [10]. For drives and traction applications, high demand of supply voltage to compensate voltage fluctuations for a brief period of time or over-speed operation of drives may be required. At that time, modulator has to go to OVM region to face those momentary issues [11].

In the OVM mode, SVPWM strategies have been extensively researched for 3 to 5-phase (5-P), 2 to 3-level converters (3-LC) since early 1990's. The OVM is utilized in induction motor (IM) drives for smooth transient operation and DC link voltage suppression [12], in SV-based low
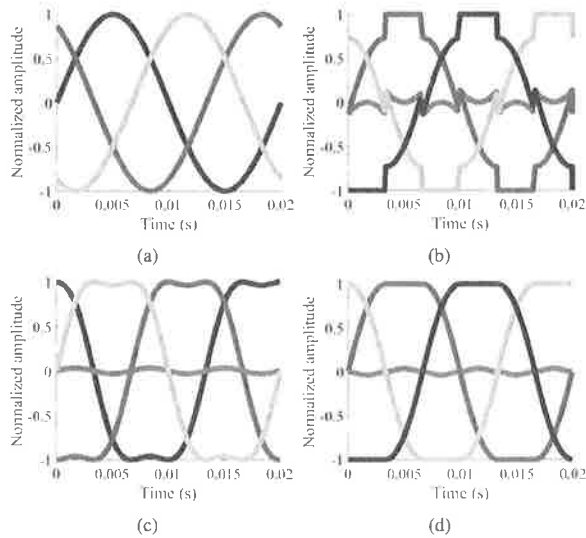
Fig. 1. Reference signals with zero sequence injection: (a) pure sinusoidal signal, (b) sinusoidal 60° bus clamped signal, (c) third harmonic injected signal, and (d) third harmonic injected 60° bus clamped signal.

Fig. 2. 5-level cascaded H-bridge converter with RL load.

frequency synchronized PWM inverter with different bus clamped PWM (BCPWM) methods [13], in 3-LC for neutral point voltage stabilization [14], in 3-LC with synchronized SVPWM technique to suppress sub-harmonics [10], and in 5-P IM drive to keep common mode voltage between 40–80% [15]. The OVM technique is also used and applied in indirect matrix converter (IMC). Three OVM schemes are proposed in [16] to improve the voltage transfer ratio (VTR) of 3 to 5-P IMC from 0.788 to 0.923, but with additional harmonics generation. All the works stated above do not focus on the overall switching performance of the converter. In [17], two OVM control methods are demonstrated, where a transition occurs from normal sinusoidal to square wave or trapezoidal signal at suitable time to improve the VTR from 0.866% to 0.97% and the efficiency up to 93.5% for IMC. A loss and efficiency analysis is included for comparison.

The OVM method is also investigated with several BCPWM schemes, mainly for 2 to 3-LCs. Some of them are shown in Fig. 1. All the BCPWM methods show linearity property with the MI until 0.907 [18]. The BCPWM can also be applied to MLC to retain high linear modulation range, high voltage gain, low switching loss, etc., particularly suitable for high speed high power drives [13]. The BCPWM schemes offer 33% less switching loss than the continuous PWM methods [19] and exhibit reduced harmonic distortion than the regular SVWPM schemes in the OVM region [13]. To carry forward the legacy of BCPWM techniques, the third harmonic injected 60° BCPWM (THSDBCPWM) and third harmonic injected 30° BCPWM (THTDBCPWM) methods were introduced recently in [20], to show better harmonic spectra than the other conventional PWM methods.

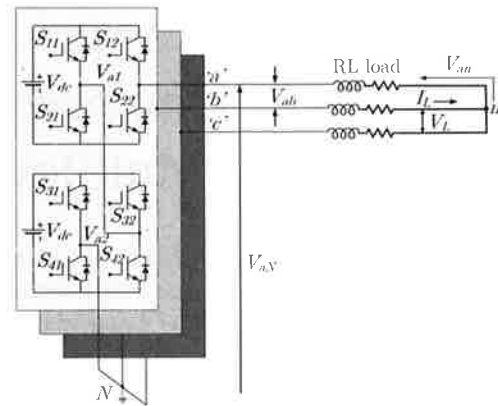Switching power losses depend on the number of semi-

conductor switches used and grow linearly with converter phase current [7]. Articles published earlier on OVM mainly focused on 2 or 3-LCs. These converters contain less number of power switches and are operated in low power range than today's MLCs. Thus, for 2 or 3-LCs, switching power losses do not pose any considerable effect on converter efficiency. However, for MV MLCs, switching losses create significant difficulties to converter overall performance. For L level 3-P converter system, $6(L - 1)$ number of power switches are needed. Choosing an optimized PWM to reduce switching losses can have paramount effect on converter performance. Therefore, this article put forth the focus on converter loss reduction in the OVM region with four types of modulators: sinusoidal PWM (SPWM), sinusoidal 60° BCPWM (SSDBCPWM), third harmonic injected PWM (THPWM) and THSDBCPWM.

II. CASCADED H-BRIDGE MULTILEVEL CONVERTER

Fig. 2, showing a 5-level CHB, has two H-bridge cells and each cell has four switches. For the first cell in phase 'a', four switches are identified as S_{11}, S_{12}, S_{21} and S_{22}. Two cells are series connected or cascaded and summation of voltages V_{a1} and V_{a2} is taken as V_{aN}. Summation of the cell voltages per phase leg can be mathematically represented as [21],

$$V_{pN} = \sum_{i=1}^{Y} V_{pi} = \sum_{i=1}^{Y} V_{dc}(S_{i1} - S_{i2}) \qquad (1)$$

where, p represents phases a, b, c and Y defines the total H-bridge cells per phase leg.

III. REGULAR PHASE DISPOSITION PWM IN OVER-MODULATION REGION

In regular phase disposition PWM (PDPWM) technique, for L level converter, $L - 1$ carrier signals should have equal peak-to-peak (p-p) amplitude A_{cr} and equal frequency,
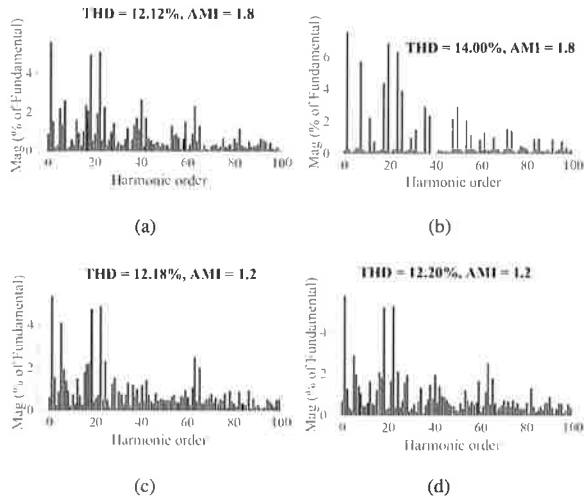
Fig. 3. Harmonic distortion for different modulations in regular OVM mode: (a) SPWM, (b) SSDBCPWM, (c) THPWM, and (d) THSDBCPWM.

so that their occupying bands remain in closed periphery [22]. The amplitude modulation index (AMI) m_a, can be calculated from (2), where A_r denotes p-p amplitude of reference signal. If m_a is taken to be 1.0, the p-p amplitude of the carrier signals can be calculated by (3) [23]. When m_a takes value greater than 1.0, the OVM mode starts in regular carrier interaction PWM.

$$m_a = \frac{A_r}{(L-1)A_{cr}} \tag{2}$$

$$A_{cr} = \frac{A_r}{(L-1)} \tag{3}$$

In Fig. 3, THD profiles using regular OVM with PDPWM technique are shown. Here, AMI for SPWM and SSD-BCPWM is taken as 1.8 and that for THPWM and THS-DBCPWM is taken as 1.2. With those AMIs, the modulator gives the best overall THD performance. Those AMIs will be particularly useful to exhibit the appropriate comparisons among the different PWM strategies with the proposed PDPWM scheme in OVM region.

IV. PROPOSED PHASE DISPOSITION PWM IN OVER-MODULATION REGION

In the proposed PDPWM in OVM method, instead of increasing the target reference signal, the contiguous carrier signal amplitudes are decreased. With the fixed reference amplitude, the normal modulator inters the OVM region. Not only this, a certain band gap between the contiguous carrier signals is introduced. This eventually helps to reduce switching loss. To do this, the amplitude of the carrier signals can be modified as,
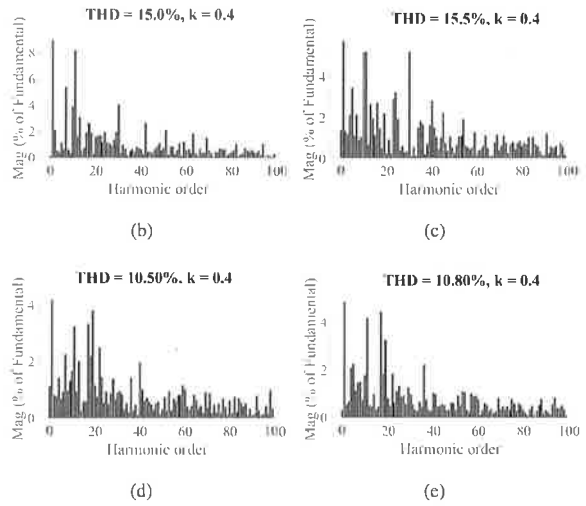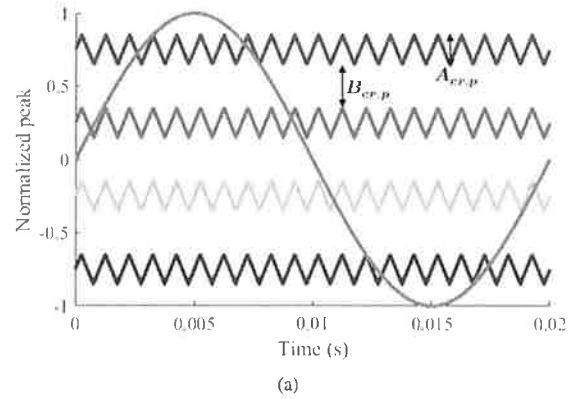
$$A_{cr,p} = \frac{kA_r}{L-1} \tag{4}$$

Fig. 4. Proposed OVM technique with harmonic distortion for different modulators: (a) proposed sinusoidal OVM technique, (b) SPWM, (c) SSD-BCPWM, (d) THPWM, and (e) THSDBCPWM.

where, $k \in R$ and $0 < k < 1$. Then the $L-1$ carrier signals are disposed by adding particular dc offset parameters in a modified way to make them remain in contiguous form as shown in Fig. 4(a) with the harmonic profiles in Figs. 4(b)–(e). The band gap $B_{cr,p}$ between two carrier signals will be,

$$B_{cr,p} = \frac{(1-k)A_r}{L-1} \tag{5}$$

The dc offset parameters can be calculated by,

$$F_n = \frac{L-2n}{L-1} \tag{6}$$

where,

$$n = 1, 2, 3 \ldots\ldots\ldots \frac{L-1}{2} \tag{7}$$

After that, they are added and subtracted correspondingly to the individual carrier signals as shown in Fig. 5. For this particular work, the target reference normalized peak is chosen as 1.00 and the variation of k offers different AMI, THD and fundamental voltage.

V. Loss Analysis of Multilevel Converter in Over-modulation Region

Loss analysis of MLC is a crucial factor as it represents the converter efficiency, reliability, cost and applicability. Therefore, a modulation method must be applied to minimize the loss of MLCs for its optimized operation. Commercial insulated gate bipolar transistor (IGBT) modules contain IGBT semiconductor switch and an anti-parallel diode. IGBT switching loss can be divided into transistor turn-on and turn-off loss with diode turn-off loss for its reverse recovery characteristics. Both IGBT and diode exhibit conduction loss. At each IGBT switching events, the energy loss will be proportional to the current level, blocking voltage (off-state voltage) and junction temperature. The average IGBT conduction loss $P_{avgC,T}$ can be calculated as [20],

$$P_{avgC,T} = \frac{1}{2\pi} \int_0^{2\pi} [v_{ce,T}(t) \times i_{c,T}(t)] \, d(\omega t) \tag{8}$$

$$= \frac{1}{2\pi} \int_0^{2\pi} [v_{cc0,T}(t)i_{c,T}(t) + R_{cc,T}i_{c,T}^2(t)] \, d(\omega t) \tag{9}$$

$$= v_{ce0,T}I_{avgC,T} + R_{cc,T}I_{rmsC,T}^2 \tag{10}$$

where, $v_{ce,T}$ and $i_{c,T}$ denote on-state collector-emitter voltage and collector currents, respectively. $v_{ce0,T}$ is on-state zero current voltage and $R_{cc,T}$ symbolizes on-state collector-emitter resistance. $I_{avgC,T}$ and $I_{rmsC,T}$ are average collector and rms currents respectively. The average conduction loss for diode $P_{avgC,D}$, can be calculated in a similar fashion as,

$$P_{avgC,D} = v_{ce0,D}I_{avgC,D} + R_{cc,D}I_{rmsC,D}^2 \tag{11}$$

where, $I_{avgC,D}$ and $I_{rmsC,D}$ denote diode average and rms currents, respectively. $v_{ce0,D}$ is diode on-state zero current voltage and $R_{cc,D}$ is the diode forward resistance. All the values can be obtained from the device data sheets. Thus, the total conduction loss per phase for $2(L-1)$ number switches in L level converter can be written as,

$$P_{cond,phase} = \sum_{i=1}^{2(L-1)} [P_{avgC,T(i)} + P_{avgC,D(i)}] \tag{12}$$

The transistor switch-on loss $P_{switchT,on}$, switch-off loss $P_{switchT,off}$ and diode turn-off loss $P_{switchD,off}$ can be determined by [20], [24],

$$P_{switchT,on} = \frac{1}{T} \frac{v_{ce,off}(t)}{v_{ce,ref}} \sum_{j=1}^{N_{T,on}} [E_{T,on(j)}(i_C(t))] \tag{13}$$

$$P_{switchT,off} = \frac{1}{T} \frac{v_{ce,off}(t)}{v_{ce,ref}} \sum_{j=1}^{N_{T,off}} [E_{T,off(j)}(i_C(t))] \tag{14}$$

$$P_{switchD,off} = \frac{1}{T} \frac{v_{D,off}(t)}{v_{ce,ref}} \sum_{j=1}^{N_{D,off}} [E_{D,off(j)}(i_D(t))] \tag{15}$$
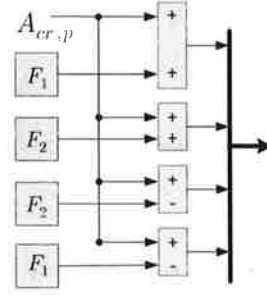

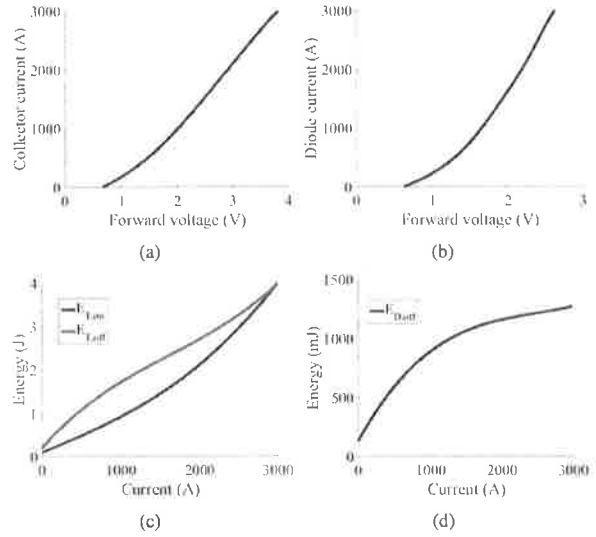Fig. 5. Phase disposed carrier signal generation for 5-level converter.

Fig. 6. Produced data sheet characteristics curves: (a) transistor on-state characteristics, (b) diode on-state characteristics, (c) transistor switching energies versus collector current, and (d) diode reverse recovery energy loss.

The switching loss energies $E_{T,on}$, $E_{T,off}$ and $E_{D,off}$ are determined by the corresponding collector current in data sheets. Here, $v_{ce,off}$, $v_{D,off}$ are instantaneous blocking voltage and $v_{ce,ref}$ is the reference blocking voltage from the device data sheet. Hence, the total loss P_{total}, can be written as,

$$P_{total} = P_{loss,T} + P_{loss,D} \tag{16}$$

where,

$$P_{loss,T} = P_{avgC,T} + P_{switchT,on} + P_{switchT,off} \tag{17}$$

$$P_{loss,D} = P_{avgC,D} + P_{switchD,off} \tag{18}$$

If P_{ouput} is termed as the converter output power, then,

$$P_{output} = \sqrt{3}V_{LL,rms}I_{ph,rms}cos(\phi) \tag{19}$$

Category (PWM)	Type	Switching loss (W)	Conduction loss (W)	THD (%)	Efficiency (%)
SPWM	AMI = 1.80	56.91	626.76	12.12	99.60
	k = 0.40	32.34	475.04	15.00	99.60
SDBCPWM	AMI = 1.80	62.30	619.00	14.00	99.60
	k = 0.40	38.37	430.00	15.50	99.59
THPWM	AMI = 1.20	58.35	630.45	12.18	99.61
	k = 0.40	32.90	604.00	10.50	99.62
THSDBCPWM	AMI = 1.20	60.41	627.02	12.20	99.61
	k = 0.40	32.34	599.63	10.80	99.62

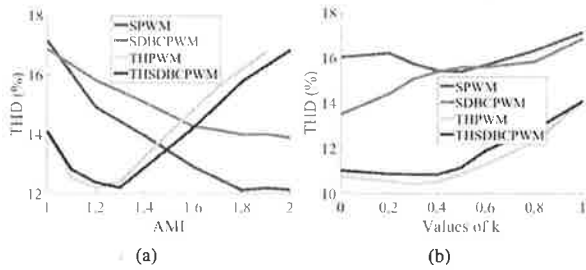Fig. 7. THD in OVM region: (a) regular and (b) proposed.

Fig. 8. Fundamental voltage in OVM region: (a) regular and (b) proposed.

where, $V_{LL,rms}$ is the line to line rms voltage, $I_{ph,rms}$ is rms phase current, and $cos(\phi)$ represents power factor of the load. The efficiency can then be calculated by,

$$\eta = \frac{P_{output}}{P_{output} + P_{total}} \qquad (20)$$
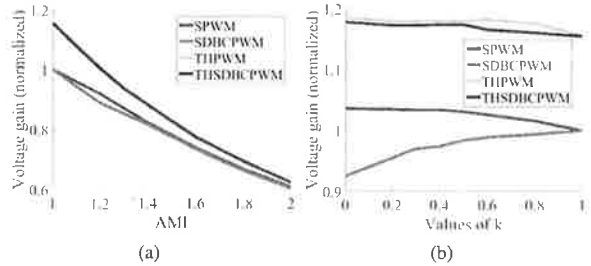
Fig. 9. Fundamental voltage gain in OVM region: (a) regular and (b) proposed.

VI. SIMULATION AND RESULTS

A 3.0 kV, 120 kW CHB 5-L converter is designed with each input cell voltage of 1.10 kV (4.0% voltage reserve) and RL load of 50 Ω and 120 mH. For switching and conduction losses calculation, each H-bridge module is considered to consist of four IGBT 5SNA1500E250300 switches (2.5 kV, 1500 A) from ASEA Brown Boverie (ABB) with 1.0 kHz switching frequency. For simulation purposes, the overall converter temperature is assumed to be 125°C. The man-ufacturer data sheet characteristic curves of IGBT module for loss calculations are approximated by the same way established in [20]. The resulting curves for diode and IGBT are shown in Fig. 6. With the simulation data, Figs. 7 to 9 are drawn and Table I is generated. From Fig. 7, it can be seen that in the regular OVM, with the increase of AMI, the THD of modulators is reduced until AMI 1.20 for THPWM and THSDBCPWM and AMI 1.80 for SPWM and SSDBCPWM. Also, the increased AMI will increase the fundamental phase voltage of the converter and will be saturated after reaching square wave mode. With proposed OVM scheme, Fig. 7(b) reveals that, with the increase of
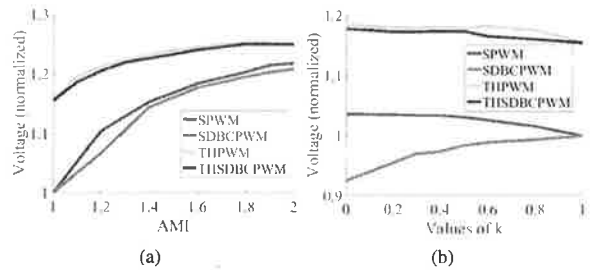
the value k, in all the modulators, THD of the output line voltage tends to decrease slightly upto $k = 0.40$ for SPWM, THPWM, THSDBCPWM and then starts to increase up to linear modulation zone. Fundamental phase voltage of the converter approximately remains the same with the variation of k for SPWM, THPWM, THSDBCPWM methods. This property is very important as it is shown in Fig. 8(b). Before advancing, definition of voltage gain G, should be given. It is the ratio of fundamental phase voltage V_{fund} and target reference V_{ref} as stated in (21).

$$G = \frac{V_{fund}}{V_{ref}} \qquad (21)$$

Fig. 9 demonstrate that G with the proposed OVM tech-nique is found to be approximately constant for SPWM, THPWM, THSDBCPWM but in the regular one, G decreases

rapidly with the increase of AMI. The highest fundamental gain in the proposed OVM approach is found to be, for SPWM is 1.037, for THPWM is 1.186, for THSDBCPWM is 1.178 and for SSDBCPWMM is less than 1.0. However, in the existing OVM method, for SPWM and SSDBCPWM, the gain is less than 1.0 and for THPWM and THSDBCPWM, the gain is less than 1.15. Therefore, G of the modulators not only increases but also remains the same within certain limit in the proposed OVM method.

Finally, Table I shows that, in every modulation techniques, switching and conduction losses are greatly reduced with comparable efficiency in the proposed OVM scheme than the existing OVM techniques. The interesting feature of the proposed scheme is that, instead of SPWM and SDBCPWM, the THD performance of THPWM and THSDBCPWM is improved than the existing ones.

VII. Conclusion

Cascaded H-bridge modular multilevel converters are highly efficient in many practical applications. Suitable number of levels, switching patterns as well as proper modulation scheme can ensure excellent converter performance. To demonstrate the efficacy of the proposed OVM technique, four types of PWM methods are considered: SPWM, SSDBCPWM, THPWM and THSDBCPWM. It is shown that the converter voltage gain is increased, the conduction and switching loss is reduced with the four types modulators in the proposed OVM method, compared to the conventional ones. THD performance also gets improved for THPWM and THSDBCPWM in the proposed OVM.

References

[1] M. R. Islam, Y. G. Guo, and J. G. Zhu, "A multilevel medium-voltage inverter for step-up-transformer-less grid connection of photovoltaic power plants," *IEEE J. Photovoltaics*, vol. 4, no. 3, pp. 881–889, 2014.

[2] H. Abu-Rub, J. Holtz, J. Rodriguez, and G. Baoming, "Medium-voltage multilevel converters—state of the art, challenges, and requirements in industrial applications," *IEEE Trans. Ind. Electron.*, vol. 57, no. 8, pp. 2581–2596, Aug 2010.

[3] M. R. Islam, Y. G. Guo, M. Jafari, Z. Malekjamshidi, and J. G. Zhu, "A 43-level 33 kV 3-phase modular multilevel cascaded converter for direct grid integration of renewable generation systems," in *2014 IEEE Innovative Smart Grid Technologies-Asia (ISGT ASIA)*, 2014, pp. 594–599.

[4] M. Marchesoni, M. Mazzucchelli, and S. Tenconi, "A non conventional power converter for plasma stabilization," in *Power Electron. Spec. Conf., 1988. PESC '88 Record., 19th Annual IEEE*, vol. 1, April 1988, pp. 122–129.

[5] J. I. Leon, S. Kouro, S. Vazquez, R. Portillo, L. G. Franquelo, J. M. Carrasco, and J. Rodriguez, "Multidimensional modulation technique for cascaded multilevel converters," *IEEE Trans. Ind. Electron.*, vol. 58, no. 2, pp. 412–420, Feb 2011.

[6] M. Malinowski, K. Gopakumar, J. Rodriguez, and M. A. Perez, "A survey on cascaded multilevel inverters," *IEEE Trans. Ind. Electron.*, vol. 57, no. 7, pp. 2197–2206, July 2010.

[7] A. M. Hava, R. J. Kerkman, and T. A. Lipo, "A high-performance generalized discontinuous PWM algorithm," *IEEE Trans. Ind. Appl.*, vol. 34, no. 5, pp. 1059–1071, Sep 1998.

[8] A. Hava, R. J. Kerkman, and T. A. Lipo, "Carrier-based PWM-VSI overmodulation strategies: analysis, comparison, and design," *IEEE Trans. Power Electron.*, vol. 13, no. 4, pp. 674–689, Jul 1998.

[9] A. Cataliotti, F. Genduso, A. Raciti, and G. R. Galluzzo, "Generalized PWM-VSI control algorithm based on a universal duty-cycle expression: Theoretical analysis, simulation results, and experimental validations," *IEEE Trans. Ind. Electron.*, vol. 54, no. 3, pp. 1569–1580, June 2007.

[10] A. R. Beig, "Synchronized SVPWM algorithm for the overmodulation region of a low switching frequency medium-voltage three-level VSI," *IEEE Trans. Ind. Electron.*, vol. 59, no. 12, pp. 4545–4554, Dec 2012.

[11] B. P. McGrath and D. G. Holmes, "Sinusoidal PWM of multilevel inverters in the overmodulation region," in *Proc. 2002 IEEE 33rd Annual IEEE Power Electron. Spec. Conf.*, vol. 2, 2002, pp. 485–490.

[12] D.-C. Lee and G.-M. Lee, "A novel overmodulation technique for space-vector PWM inverters," *IEEE Trans. Power Electron.*, vol. 13, no. 6, pp. 1144–1151, Nov 1998.

[13] G. Narayanan and V. T. Ranganathan, "Extension of operation of space vector PWM strategies with low switching frequencies using different overmodulation algorithms," *IEEE Trans. Power Electron.*, vol. 17, no. 5, pp. 788–798, Sep 2002.

[14] A. K. Gupta and A. M. Khambadkone, "A simple space vector PWM scheme to operate a three-level NPC inverter at high modulation index including overmodulation region, with neutral point balancing," *IEEE Trans. Ind. Appl.*, vol. 43, no. 3, pp. 751–760, May 2007.

[15] M. J. Durn, J. Prieto, and F. Barrero, "Space vector PWM with reduced common-mode voltage for five-phase induction motor drives operating in overmodulation zone," *IEEE Trans. Power Electron.*, vol. 28, no. 8, pp. 4030–4040, Aug 2013.

[16] M. Chai, D. Xiao, R. Dutta, and J. E. Fletcher, "Space vector PWM techniques for three-to-five-phase indirect matrix converter in the overmodulation region," *IEEE Trans. Ind. Electron.*, vol. 63, no. 1, pp. 550–561, Jan 2016.

[17] G. T. Chiang and J. I. Itoh, "Comparison of two overmodulation strategies in an indirect matrix converter," *IEEE Trans. Ind. Electron.*, vol. 60, no. 1, pp. 43–53, Jan 2013.

[18] A. M. Hava, R. J. Kerkman, and T. A. Lipo, "Simple analytical and graphical methods for carrier-based PWM-VSI drives," *IEEE Trans. Power Electron.*, vol. 14, no. 1, pp. 49–61, Jan 1999.

[19] K. Zhou and D. Wang, "Relationship between space-vector modulation and three-phase carrier-based PWM: a comprehensive analysis," *IEEE Trans. Ind. Electron.*, vol. 49, no. 1, pp. 186–196, Feb 2002.

[20] M. R. Islam, A. M. Mahfuz-Ur-Rahman, M. M. Islam, Y. G. Guo, and J. G. Zhu, "A modular medium voltage grid connected converter with improved switching techniques for solar photovoltaic systems," *IEEE Trans. Ind. Electron.*, 2017, in press.

[21] J. Rodríguez, S. Bernet, B. Wu, J. O. Pontt, and S. Kouro, "Multilevel voltage-source-converter topologies for industrial medium-voltage drives," *IEEE Trans. Ind. Electron.*, vol. 54, no. 6, pp. 2930–2945, 2007.

[22] G. Carrara, S. Gardella, M. Marchesoni, R. Salutari, and G. Sciutto, "A new multilevel PWM method: A theoretical analysis," *IEEE Trans. Power Electron.*, vol. 7, no. 3, pp. 497–505, 1992.

[23] M. R. Islam, Y. G. Guo, and J. G. Zhu, "A high-frequency link multilevel cascaded medium-voltage converter for direct grid integration of renewable energy systems," *IEEE Trans. Power Electron.*, vol. 29, no. 8, pp. 4167–4182, Aug 2014.

[24] S. Rohner, S. Bernet, M. Hiller, and R. Sommer, "Modulation, losses, and semiconductor requirements of modular multilevel converters," *IEEE Trans. Ind. Electron.*, vol. 57, no. 8, pp. 2633–2642, Aug 2010.